



OPEN

A neural network computational structure for the fractional order breast cancer model

Zhenglin Huang¹✉, Qusain Haider^{2,3}, Zulqurnain Sabir⁴, Mubashar Arshad^{2,3,5}✉, Bushra Khatoon Siddiqui⁶ & Mohammad Mahtab Alam⁷

The current study provides the numerical performances of the fractional kind of breast cancer (FKBC) model, which are based on five different classes including cancer stem cells, healthy cells, tumor cells, excess estrogen, and immune cells. The motive to introduce the fractional order derivatives is to present more precise solutions as compared to integer order. A stochastic computing reliable scheme based on the Levenberg Marquardt backpropagation neural networks (LMBNNS) is proposed to solve three different cases of the fractional order values of the FKBC model. A designed dataset is constructed by using the Adam solver in order to reduce the mean square error by taking the data performances as 9% for both testing and validation, while 82% is used for training. The correctness of the solver is approved through the negligible absolute error and matching of the solutions for each model's case. To validate the accuracy, and consistency of the solver, the performances based on the error histogram, transition state, and regression for solving the FKBC model.

There are various dangerous diseases among them breast cancer (BC) is one of the serious global health issues, which is commonly found in the women throughout the world. The breast's epidermal cells are the first to become cancerous tumors, which can then spread to other parts of the human organism or attack tissues that are nearby. BC can develop in the breast's lobes or in the inner ducts layer that produce milk, which is documented as lobular carcinoma or ductal carcinoma¹. Several mathematical frameworks have been created over the investigations of BC to learn more about how it develops and potential treatments. This cancer also occurred in male with rare cases with the rate of occurrence of 0.5% to 1% as compared to female BC²⁻⁵.

BC is considered more complicated in women as compared to men and the chances of recovery in men are high in comparison with the females⁶. The detailed study based on the connection of male and female BC is presented by Miao⁷. Those women who are married with close relatives can have higher chances of BC. Couch⁸ highlighted the importance of breast cancer based on the susceptibility genes using the large triple-negative BC cohort unselected based on the family history of BC. It is the second most invasive cancer worldwide that wrapped around 2 million new people into positive cases each year. This high number takes into the dangerous zone, which is required to have a need for better preventative measures, early diagnosis techniques, and cutting-edge therapeutic approaches. BC produces various risk factors including those connected to reproduction, hormones, obesity, and a favorable family history. The difference between early and late stages of the BC is dependent on the age-specific incidence rates⁹. Fan et al.¹⁰ discussed the mathematical models using the bioinformatical and computational studies, which help to monitor the damage of Deoxyribonucleic acid recognition, tumor growth, chromatin remodeling, cellular distribution, and checkpoint regulator. Mufudza et al.¹¹ discussed the organizational impacts of all known single nucleotide polymorphisms or genetic variants in the breast cancer genes. The initial stage of BC creates the physical irregularity can be controlled by using the good treatment and early detection is crucial based on the effective measures of the disease. Bray et al.¹² provided the several risk factors including the reproduction, hormones, obesity, and a favorable family history with the role in BC development. Arshad et al.¹³ described the pathogenic mutations with a high propensity to produce cancer located areas of the gene.

¹North China Institute of Computing Technology, Beijing 100000, China. ²Department of Mathematics, University of Gujrat, Gujrat 50700, Pakistan. ³Institute for Numerical and Applied Mathematics, University of Göttingen, 37083 Göttingen, Germany. ⁴Department of Computer Science and Mathematics, Lebanese American University, Beirut, Lebanon. ⁵Department of Mathematics, Abbottabad University Science and Technology, Abbottabad 22500, Pakistan. ⁶Department of Mathematics, COMSATS University Islamabad, Wah Campus, Wah Cantt 47040, Pakistan. ⁷Department of Basic Medical Sciences, College of Applied Medical Science, King Khalid University, 61421 Abha, Saudi Arabia. ✉email: Hzl_2970558385@163.com; imbashrii@gmail.com

There are various studies that highlights the importance of genetic profiling based on BC prevention and its therapy by illuminating the role of genes using a predisposing individual of the illness^{1,14,15}. Most pathogenic mutations with a high propensity to cause cancer are areas of the gene. Genes play a key role in the development of BC using the increase of estrogen level, which causes a natural body response toward growing the tumors in the BC dynamics¹⁶. Enderling et al.¹⁷ presented the mathematical cancerous cell model using the regulated healthy pre-cancerous cells formed in the post-pubertal BC structure. BC development with higher estrogen levels is studied with the impacts of healthy breast epithelial cells, interactions among cancer cells, the body's natural immune response, and non-proliferative tumor cells¹⁸.

Mathematical systems are important tools in numerous fields of engineering, science, and economics. There are several mathematical models that have been studied in current decades and the solution of these models have been presented by using different schemes. To mention a few of them, Ganji et al.¹⁹ presented the solutions of the brain tumor model using the fractional operator. Sánchez et al.²⁰ provided the solutions of the coronavirus model by applying a reliable numerical scheme. Sabir et al.²¹ provided the results of prediction differential system by using the explicit Runge–Kutta and Adams numerical techniques. Hart et al.²² discussed the mathematical modelling of the functionally dependent bone remodeling and provided its numerical solutions. Fogelson et al.²³ designed and studied numerically by using a mathematical system based on the platelet adhesion and aggregation during blood clotting. Sana et al.²⁴ discussed a mathematical model based on the supply chain systems. The coronavirus time series data by applying the spectral analysis and deep learning methods have been proposed by Oshinubi et al.²⁵. Few recent mathematical models that have been used to solve with different numerical schemes are provided in these references^{26–28}.

The purpose of this research is to obtain the solutions of the fractional kind of breast cancer (FKBC) system in order to get more precise solutions as compared to integer order. Hence, a reliable stochastic scheme based on the Levenberg Marquardt backpropagation neural networks (LMBNNs) is proposed for the FKBC model. The stochastic process has been derived before to solve various kind of the mathematical model, but the solutions of the FKBC model have been presented first time with the implementation of this scheme. Currently, the neural network-based procedures have been used to solve functional form of singular models²⁹, hepatitis virus models³⁰, bone remodeling model³¹, fractional vector-host diseased model³², SIRC epidemic model³³, Zika virus model³⁴, breathing transmission system³⁵, thermal explosion model³⁶, Rabinovich–Fabrikant system³⁷, Layla and Majnun model³⁸ and food chain model³⁹.

The fractional order models are considered more challenging and provide more reliable results to solve the differential model. Fractional types of derivatives are implemented to test the effectiveness of the real-world applications^{16,17}. Over the past 3 decades, the implementation of fractional calculus has been observed widely by applying the powerful operators of Weyl–Riesz¹⁸, Caputo¹⁹, Riemann–Liouville²⁰, Erdelyi–Kober²¹, and Grnwald–Letnikov²². The Caputo derivative can be applied to solve both conditions of the model homogeneous and non-homogeneous. All these operators have their own drawbacks; however, the Caputo derivatives are considered simple as compared to other operators. Some novel motivations of this study are given as:

- The design of the FKBC system have been provided and the solutions have been performed by using the LMBNNs.
- Three different cases based on the fractional order have been presented to solve the FKBC system.
- The correctness of the scheme is observed by using the overlapping of the outputs.
- The absolute error (AE) results in good performances enhance the reliability of the proposed solver.

The other paper's parts are organized as: Sect. "Mathematical FKBC system" describes the construction of the FKBC system, Sect. "Designed LMBNNs procedure" provides the proposed technique based LMBNNs, Sect. "Results and discussions" is constructed based on the calculated outcomes, while conclusions are proposed in Sect. "Conclusions".

Mathematical FKBC system

This section provides the FKBC system, which is divided into five different categories named as cancer stem cells $C(t)$, tumor cells $T(t)$, healthy cells $H(t)$, immune cells $I(t)$, and excess estrogen $E(t)$. The mathematical form of the integer order BC model is given as¹⁶:

$$\left\{ \begin{array}{l} \frac{dC(t)}{dt} = k_1 C(t) \left(1 - \frac{C(t)}{M_1} \right) - \gamma_1 C(t)I(t) + \frac{p_1 E(t)C(t)}{a_1 + C(t)}, \\ \frac{dT(t)}{dt} = k_2 C(t) \left(\frac{C(t)}{M_1} \right) \left(1 - \frac{T(t)}{M_2} \right) - n_1 T(t) - \gamma_2 T(t)I(t) + \frac{p_2 T(t)E(t)}{a_2 + T(t)}, \\ \frac{dH(t)}{dt} = q \left(1 - \frac{H(t)}{M_3} \right) H(t) - \delta T(t)H(t) - \frac{p_3 E(t)H(t)}{a_3 + H(t)}, \\ \frac{dI(t)}{dt} = s + \frac{\rho I(t)T(t)}{T(t) + w} - \gamma_3 T(t)I(t) - n_2 I(t) - \frac{u E(t)I(t)}{E(t) + v}, \\ \frac{dE(t)}{dt} = \tau - \left(\mu + \frac{d_1 C(t)}{C(t) + a_1} + \frac{d_2 T(t)}{T(t) + a_2} + \frac{d_3 H(t)}{H(t) + a_3} \right), \end{array} \right. \quad (1)$$

where k_1, k_2 and q denote the normal rate of cell separation for first three dynamics, and M_1 indicates the carrying size based on the cells of first three dynamics. The rates at which estrogen promotes the growth of cancer stem

and tumor cells, as well as the rates at which healthy cells are lost because of estrogen-induced DNA mutation, are shown in p_1 , p_2 , and p_3 , respectively. It is also presented the rates at which immune cells react to tumor cells and cancer stem cells; a_1 , a_2 , and a_3 designate the number of first three dynamics. The values of n_1 and n_2 are the usual tumor. In addition, the rate at which healthy cells decease, s also shows the basis rate of resistant cells. u is the rate of immunological suppression caused by estrogen; v is the immune cell threshold; The letters τ stands the continuous estrogen infusion, the body's estrogen washout rate, and the letters d_1 , d_2 and d_3 are the rates at which cancer stem cells, tumor cells, and healthy cells absorb estrogen, respectively. The fractional form of the above system becomes as Ref. ¹⁶.

$$\begin{cases} \frac{d^\alpha C(t)}{dt^\alpha} = k_1 C(t) \left(1 - \frac{C(t)}{M_1}\right) - \gamma_1 C(t)I(t) + \frac{p_1 E(t)C(t)}{a_1 + C(t)}, \\ \frac{d^\alpha T(t)}{dt^\alpha} = k_2 C(t) \left(\frac{C(t)}{M_1}\right) \left(1 - \frac{T(t)}{M_2}\right) - n_1 T(t) - \gamma_2 T(t)I(t) + \frac{p_2 E(t)T(t)}{a_2 + T(t)}, \\ \frac{d^\alpha H(t)}{dt^\alpha} = q H(t) \left(1 - \frac{H(t)}{M_3}\right) - \delta T(t)H(t) - \frac{p_3 E(t)H(t)}{a_3 + H(t)}, \\ \frac{d^\alpha I(t)}{dt^\alpha} = s + \frac{\rho I(t)T(t)}{w + T(t)} - \gamma_3 T(t)I(t) - n_2 I(t) - \frac{u E(t)I(t)}{v + E(t)}, \\ \frac{d^\alpha E(t)}{dt^\alpha} = \tau - \left(\mu + \frac{d_1 C(t)}{a_1 + C(t)} + \frac{d_2 T(t)}{a_2 + T(t)} + \frac{d_3 H(t)}{a_3 + H(t)}\right), \end{cases} \quad (2)$$

where α stands the fractional order Caputo derivative. To investigate the complicated features, such as super slow evolution and superfast transients are considered challenging as compared to integer order given in system (1). There are various recent applications, where the fractional kind of the derivatives have been used. Some of them are inconsistent heat transmission⁴⁰, pine wilt disease model with convex rate⁴¹, spatiotemporal outlines⁴², and soil animal approximation⁴³, and soil animal constituent content⁴⁴.

Designed LMBNNs procedure

The stochastic computational performances based on the LMBNNs scheme to solve the mathematical FKBC system as stated in the set of systems (2) is provided in this section. Three components of model using the developed technique, and outcomes are provided in Fig. 1a and b. These Figs depict the workflow diagram for the FKBC system. The design presentations are described in two different metrics including LMBNNs-based processes and the mathematical process. The design of the dataset is presented by using the Adam scheme and the division of the data contains 82% (training) and 9% for both verification and testing by taking 15 hidden neurons. Log-sigmoid transfer function in the hidden layers is selected and single input and output layer structure based on the neurons is obtained. The current neural network study is operated with untimely conjunction, overfitting, and concealed scenarios. Therefore, the parameters of the networks have been used carefully after considerable tests, experience, and knowledge. A fully concentration is required to adjust the parameter setting and a small modification in the setting can change the whole scenario and can impact the performance of the investigations. The "MATLAB" software (NFTOOL command) is used to implement the stochastic process based on the LMBNNs, which include the correct hidden neuron sections, testing statistics, learning strategies, and verification statics. Table 1 shows the parameter setting to perform the LMBNNs for solving the FKBC model.

Results and discussions

In this section, three different cases have been taken by using the values of $\alpha = 0.5, 0.7$ and 0.9 for solving the mathematical model.

Analysis of results for case 1

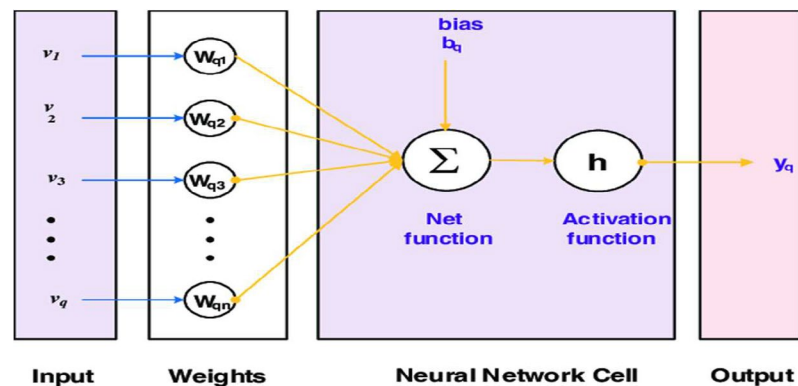
Consider the values $\alpha = 0.5$, $k_1 = 0.05$, $M_1 = 0.02$, $p_1 = 0.005$, $a_1 = 0.6$, $\gamma_1 = 0.01$, $p_2 = 0.01$, $a_2 = 0.07$, $k_2 = 0.02$, $M_2 = 0.5$, $\gamma_2 = 0.1$, $n_1 = 0.3$, $q = 0.3$, $M_3 = 0.4$, $p_3 = 0.5$, $a_3 = 0.5$, $\delta = 0.05$, $s = 0.02$, $n_2 = 0.005$, $\gamma_3 = 0.6$, $u = 0.01$, $v = 0.01$, $\rho = 0.07$, $\omega = 0.02$, $\tau = 0.5$, $\mu = 0.1$, $d_1 = 0.3$, $d_2 = 0.3$, $d_3 = 0.5$ in Eq. (2), while the values of the initial conditions have been selected 1.2 for each class.

The mean square error (MSE) and state evolution (SE) results of the FKBC model's performance are shown in Fig. 2a,b for case 1. The first two parts of the Fig. 2 indicate the decrement of MSE for solving the FKBC model. The best validation performances are reported as 3.4006×10^{-9} , while the gradient is reported as 1.4903×10^{-6} , and the epochs have been calculated for this case are 220. Figure 3 shows the function fit and error histogram (EH) performances for case 1. The first half is designed based on the func fit, while the second half provides the EH. The values of the EH are presented as 5.95×10^{-5} . Figure 4 provides the regression performances for case 1, which is calculated as 1 that shows the perfect model.

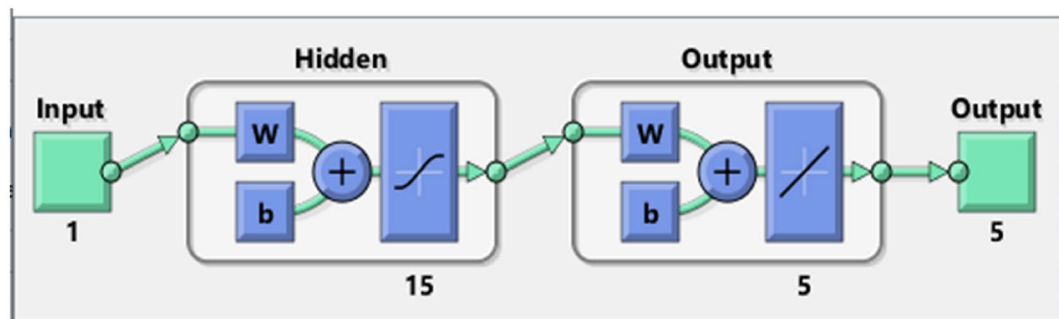
Analysis of results for case 2

Consider $\alpha = 0.7$, $k_1 = 0.05$, $M_1 = 0.02$, $p_1 = 0.005$, $a_1 = 0.6$, $\gamma_1 = 0.01$, $p_2 = 0.01$, $a_2 = 0.07$, $k_2 = 0.02$, $M_2 = 0.5$, $\gamma_2 = 0.1$, $n_1 = 0.3$, $q = 0.3$, $M_3 = 0.4$, $p_3 = 0.5$, $a_3 = 0.5$, $\delta = 0.05$, $s = 0.02$, $n_2 = 0.005$, $\gamma_3 = 0.6$, $u = 0.01$, $v = 0.01$, $\rho = 0.07$, $\omega = 0.02$, $\tau = 0.5$, $\mu = 0.1$, $d_1 = 0.3$, $d_2 = 0.3$, $d_3 = 0.5$ in Eq. (2), while the values of the initial conditions have been selected 1.2 for each class.

The values of the MSE and SE to present the FKBC model's performance are illustrated in Fig. 5a,b for case 2. The first two half of Fig. 5 represent the decrement of MSE for solving the FKBC model. The best validation



(a) A general structure of a single neuron



(b) A layer structure of the model

Figure 1. (a) A general structure of a single neuron. (b) A layer structure of the model.

Index	Settings
Activation function	Log-sigmoid
Fitness goal (MSE)	0
Minimum gradient	10^{-7}
Maximum Mu values	10^{10}
Hidden neurons	15
Maximum Epochs	1000
Output layer	Single
Increasing Mu performances	10
Validation statics	9%
Authentication fail amount	6
Lower Mu values	0.1
Sample assortment	Arbitrary
Training data	82%
Adaptive parameter	7×10^{-5}
Testing data	9%
Input layer	Single
Dataset	Adam technique
Adam solver implementations	Default
Stoppage criteria	Default

Table 1. Parameters adjustment to perform the LMBNNs.

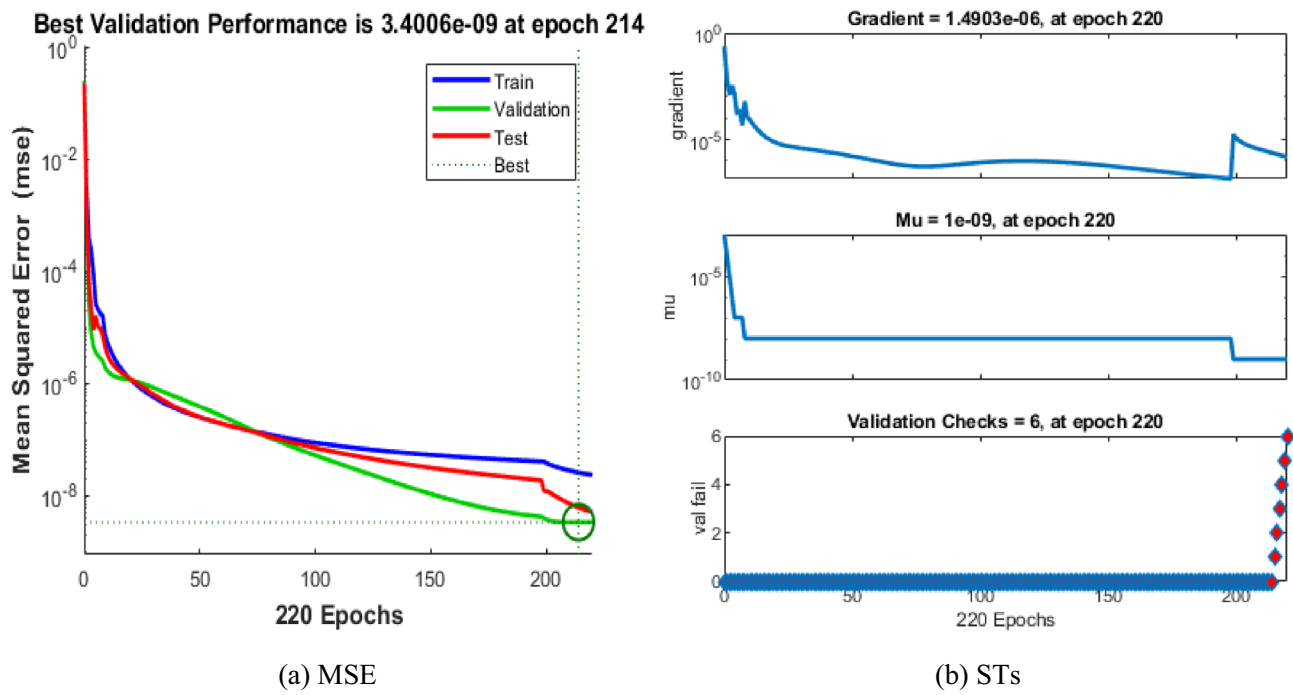


Figure 2. MSE and STs for the FKBC system based case 1.

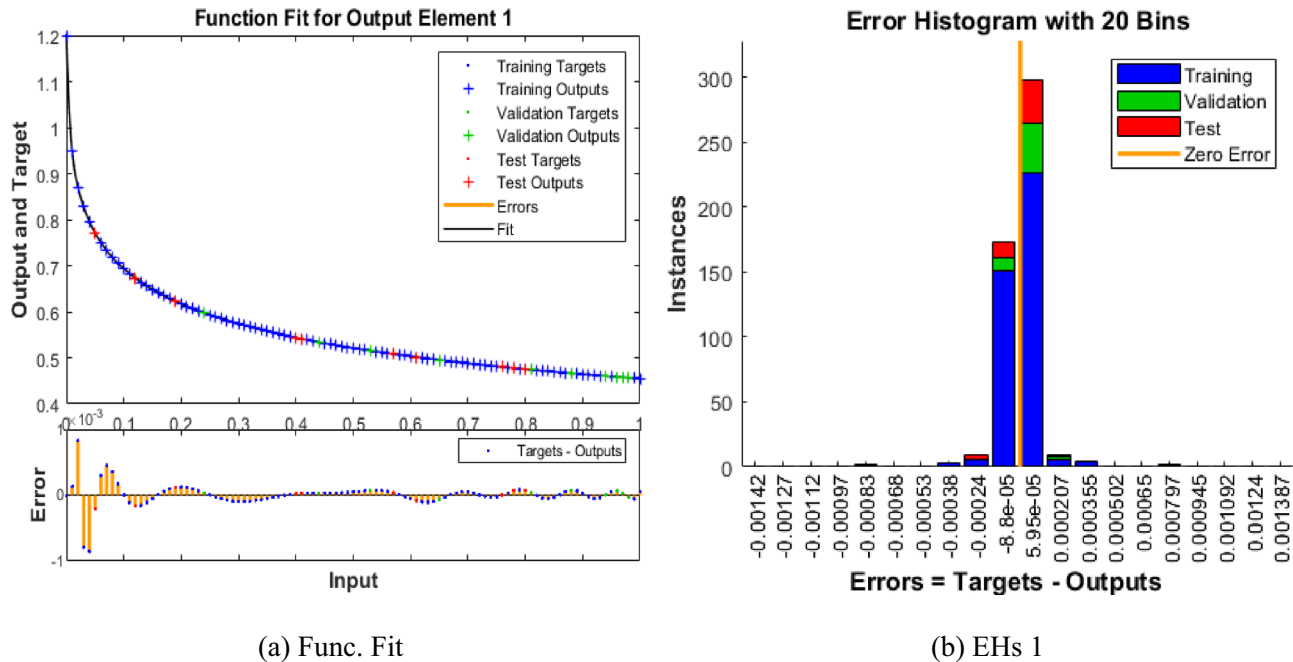


Figure 3. Func fit and EHs for the mathematical system for case 1.

performances are reported as 3.8361×10^{-9} , while the gradient is reported as 7.271×10^{-6} , and the epochs have been calculated for this case are 144. Figure 6 shows the function fit and EH performances for case 2. The first half is designed based on the func fit, while the second half provides the EH. The values of the EH are presented as 3.93×10^{-6} . Figure 7 describes the regression for case 2, which is performed as 1 that represents the perfect model.

Analysis of results of case 3

Consider $\alpha = 0.9$, $k_1 = 0.05$, $M_1 = 0.02$, $p_1 = 0.005$, $a_1 = 0.6$, $\gamma_1 = 0.01$, $p_2 = 0.01$, $a_2 = 0.07$, $k_2 = 0.02$, $M_2 = 0.5$, $\gamma_2 = 0.1$, $n_1 = 0.3$, $q = 0.3$, $M_3 = 0.4$, $p_3 = 0.5$, $a_3 = 0.5$, $\delta = 0.05$, $s = 0.02$, $n_2 = 0.005$, $\gamma_3 = 0.6$,

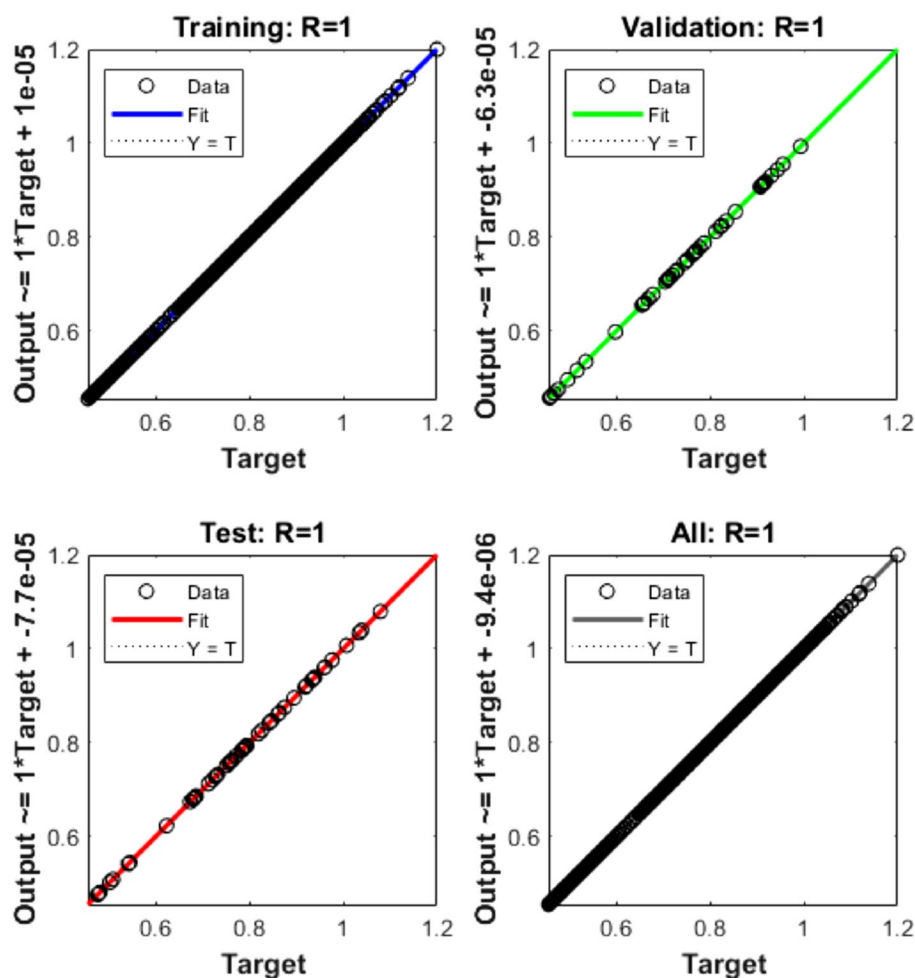


Figure 4. Regression for the FKBC model (1).

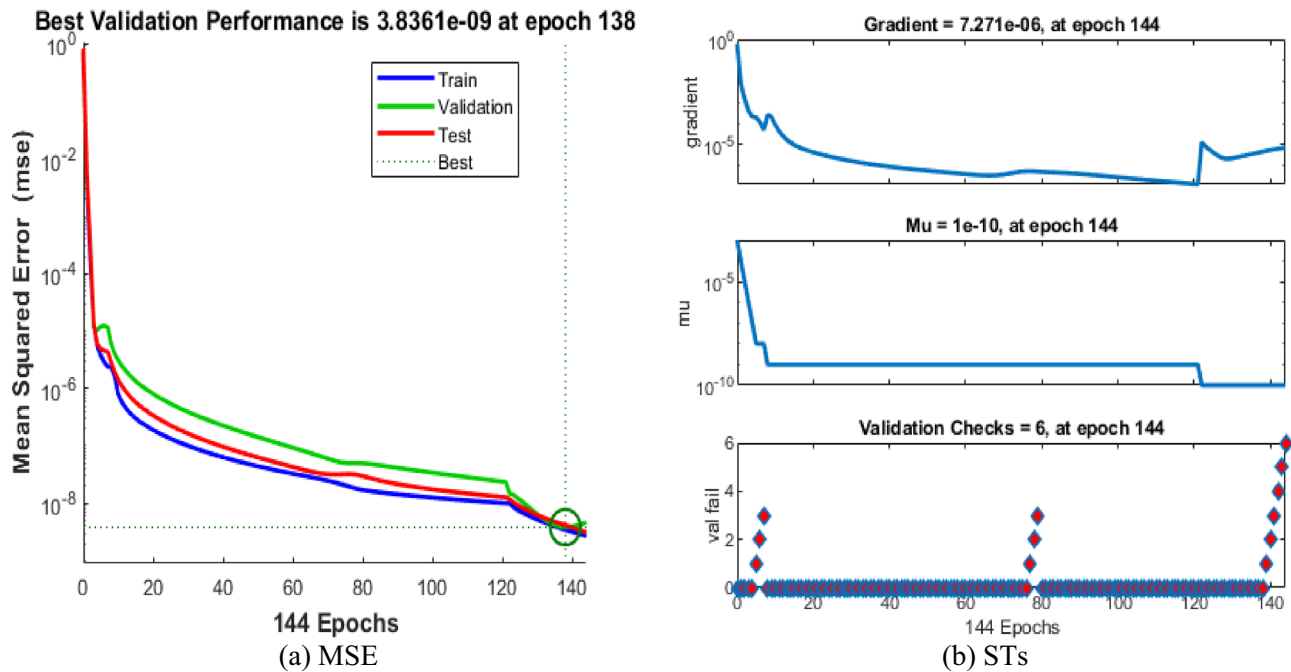


Figure 5. MSE and STs for the FKBC system for case 2.

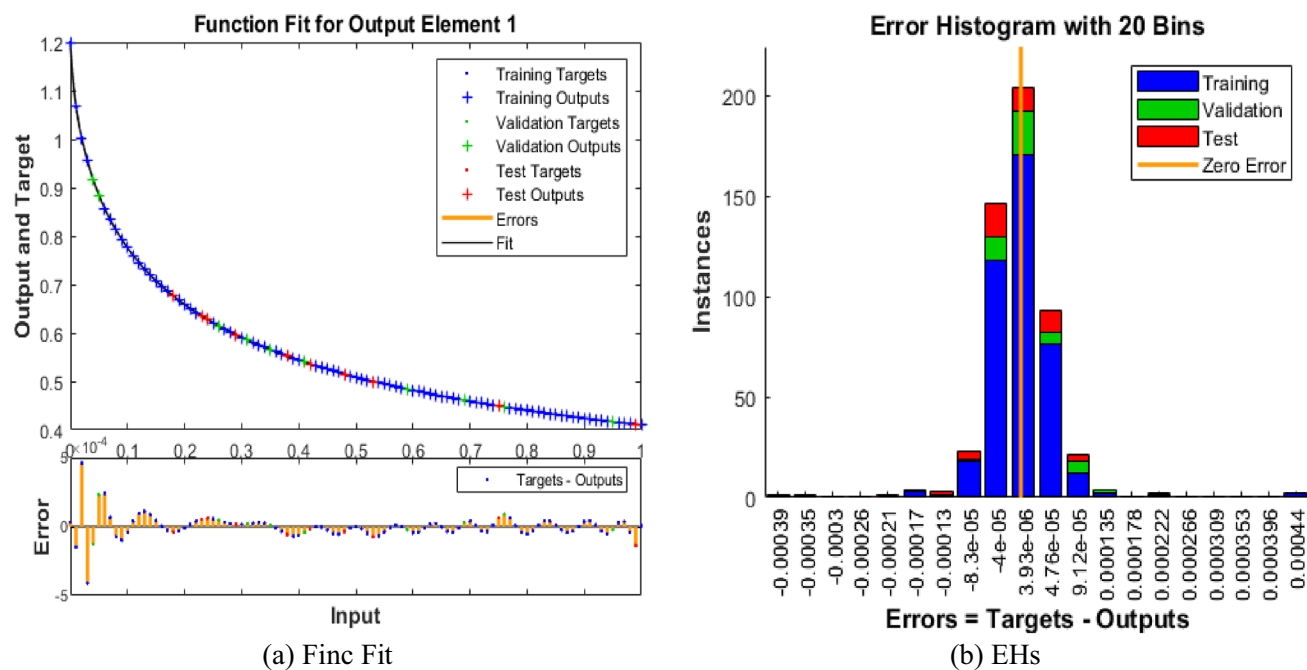


Figure 6. Func fit and EHs for the mathematical system based case 2.

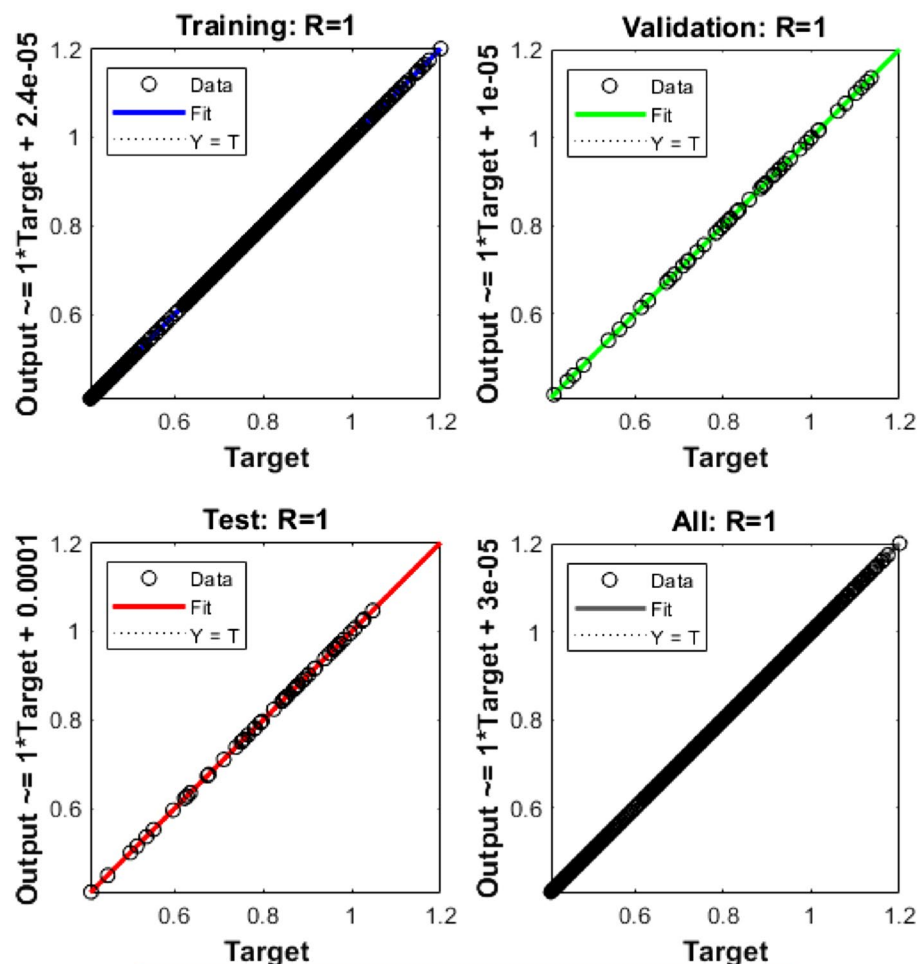


Figure 7. Regression for the FKBC model (2).

$u = 0.01, v = 0.01, \rho = 0.07, \omega = 0.02, \tau = 0.5, \mu = 0.1, d_1 = 0.3, d_2 = 0.3, d_3 = 0.5$ in Eq. (2), while the values of the initial conditions have been selected 1.2 for each class.

The values of the MSE and SE to present the FKBC model's performance are demonstrated in Fig. 8a,b for case 3. The first two half of Fig. 8 represent the decrement of MSE for solving the FKBC model. The best validation performances are reported as 1.5709×10^{-9} , while the gradient is reported as 1.6598×10^{-6} , and the epochs have been calculated for this case are 144. Figure 9 shows the function fit and EH performances for case 3. The first half is designed based on the func fit, while the second half provides the EH. The values of the EH are presented as 1.33×10^{-5} . Figure 10 describes the regression for case 3, which is performed as 1 that represents the perfect model.

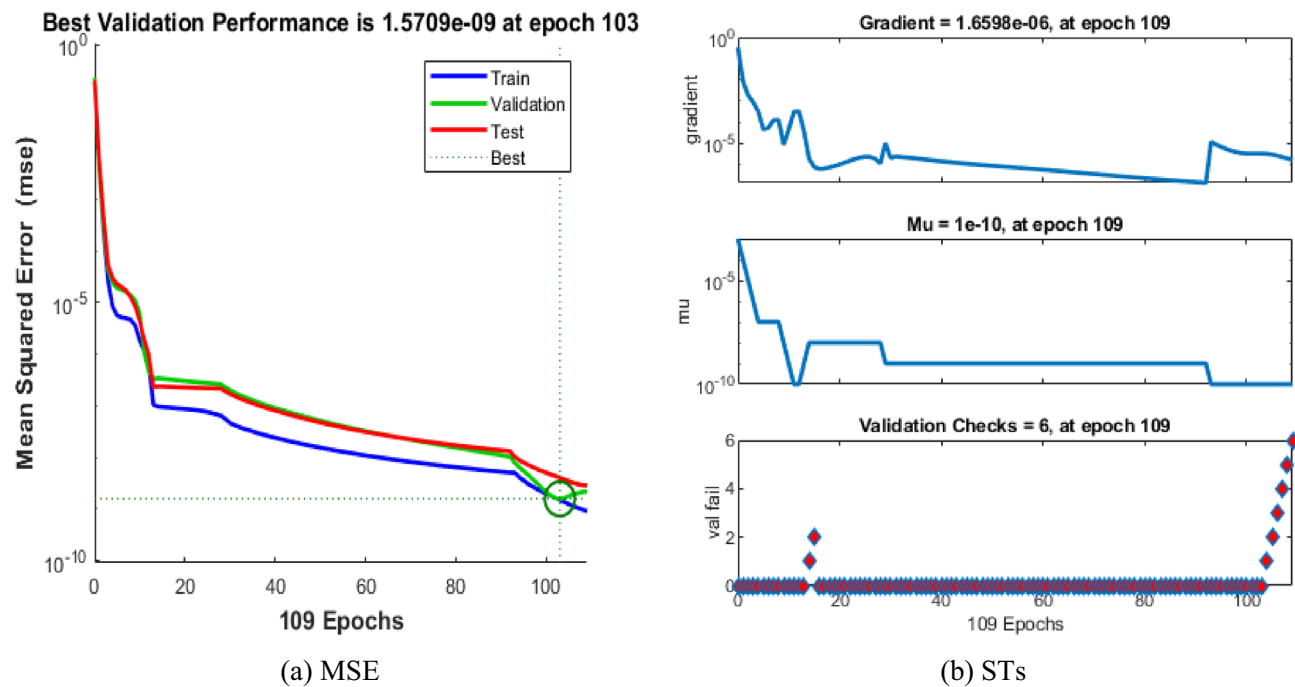


Figure 8. MSE and STs performances for the FKBC system for case 2.

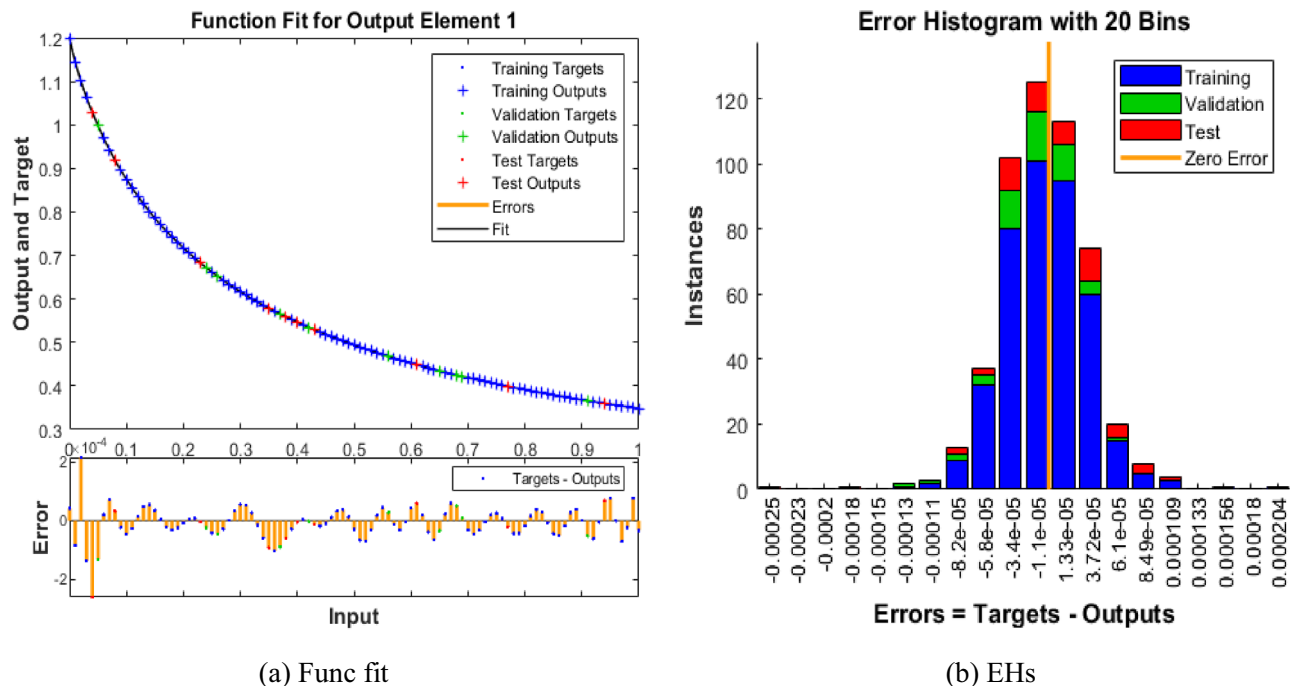


Figure 9. Func fit and EHs for the FKBC system for case 3.

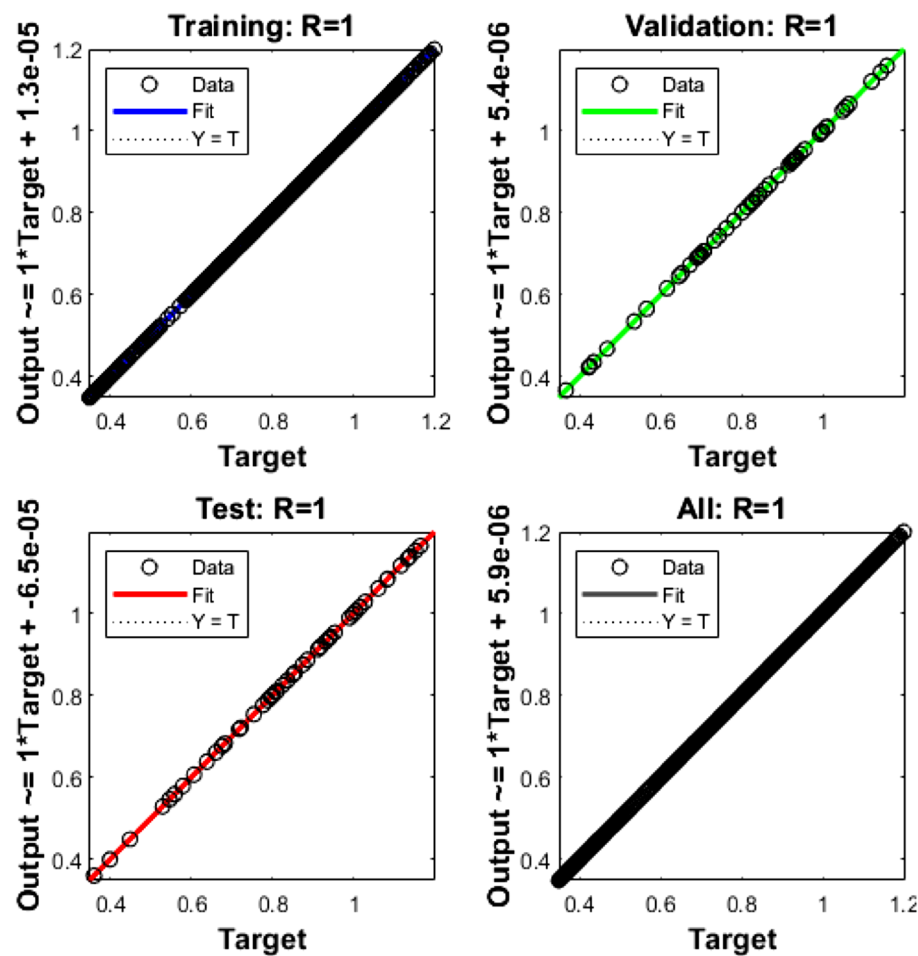


Figure 10. Regression for the FKBC model (3).

The AE is reported in Fig. 11, which shows that these values are performed as 10^{-04} to 10^{-06} for each dynamic of the model. This negligible AE performance enhance the correctness of the scheme. For the solution of the FKBC model using the procedures based on the LMBNNs are presented in Fig. 12. It is reported that the matching of the results is obtained for each case of the FKBC system.

Table 2 shows the MSE performances based on the neural networks along with the counted epochs and complexity measures.

Conclusions

In this study, the numerical solution of the fractional breast cancer system have been presented, which are based on five different classes including cancer stem cells, healthy cells, tumor cells, excess estrogen, and immune cells. Some of the concluding remarks of this work are given as:

- The fractional derivatives have been introduced to solve the breast cancer mathematical model.
- The fractional kind of derivatives have been provided to get more precise solutions of the model as compared to integer order.
- A stochastic computing Levenberg Marquardt backpropagation neural networks scheme has been proposed for three fractional order cases of the FKBC model.
- The constructions of the designed dataset based on the Adam solver has been presented to reduce the MSE by taking the data performances as 9% for both testing and validation, while 82% is used for training.
- The correctness of the solver has been approved through the negligible absolute error along with the matching of the solutions for each model's case.
- To authenticate the accuracy of the solver, the performances based on the error histogram, transition state, and regression for solving the FKBC model has been provided.

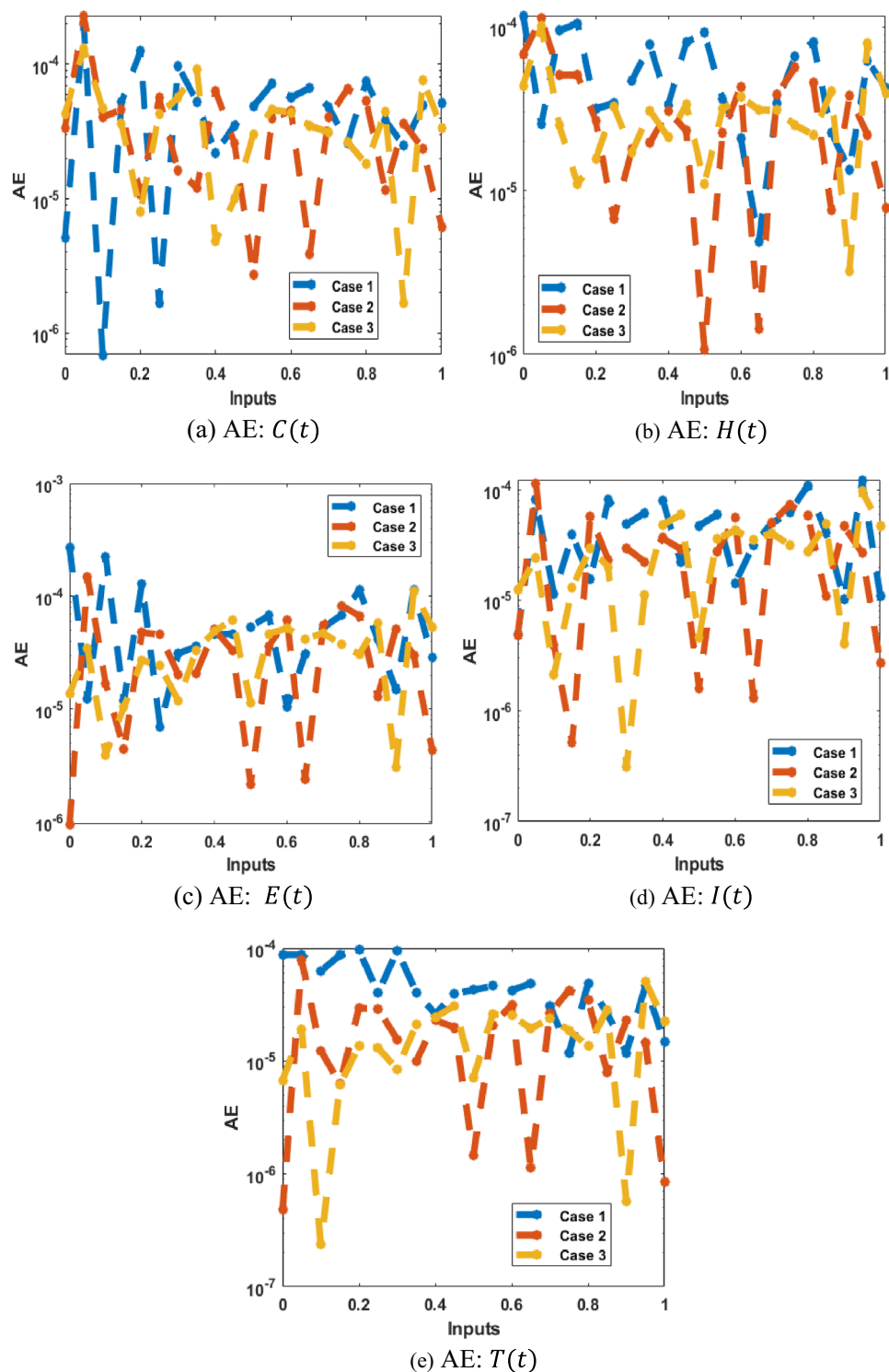


Figure 11. (a–e) AE values for the FKBC model.

Future recommendations

The designed structure based on the stochastic approach can be executed for various nonlinear natured models^{45–62}.

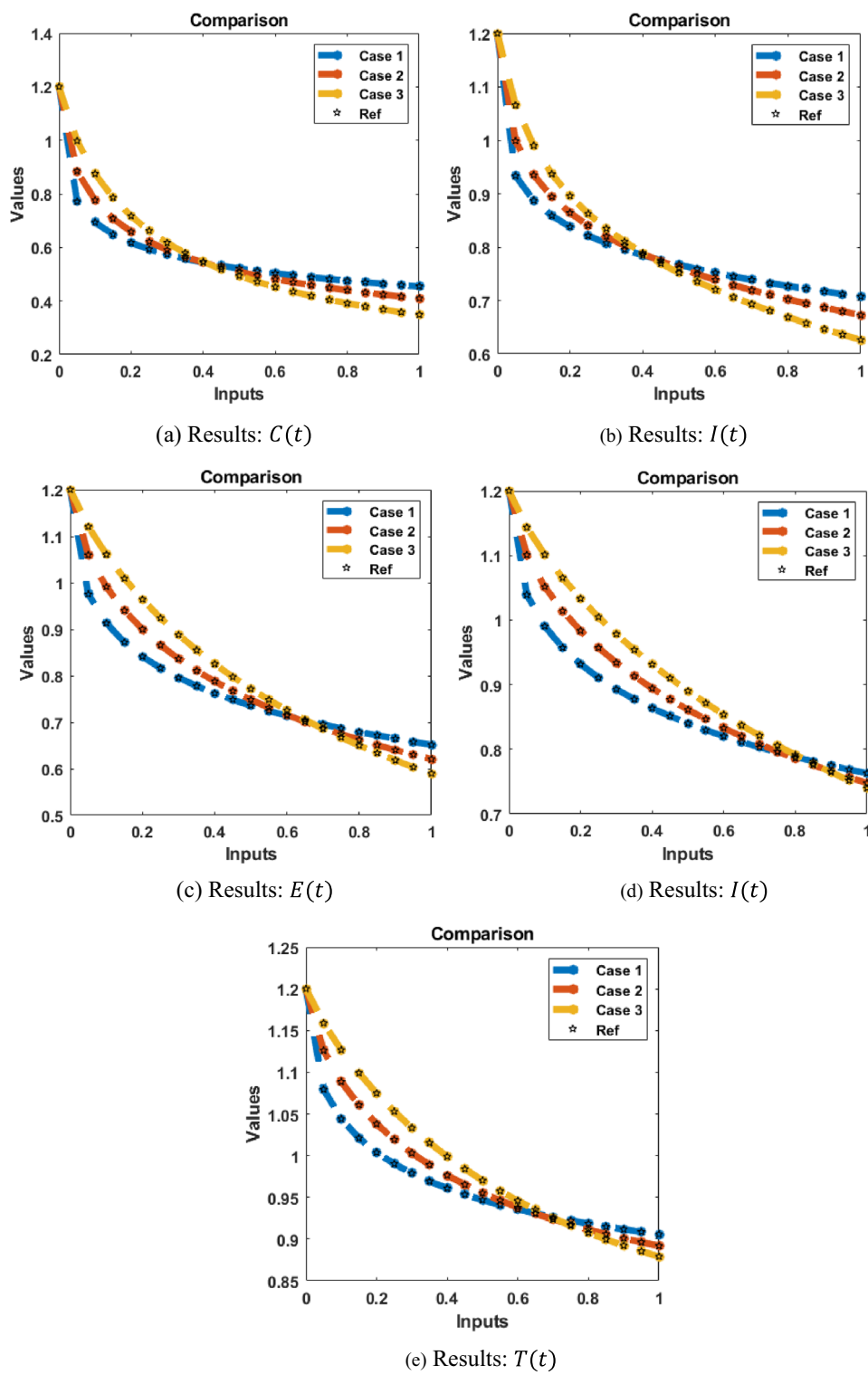


Figure 12. (a–e) Result assessment for the FKBC model.

Case	MSE			Performance	Gradient	Mu	Epoch	Time
	[Training]	[Verification]	[Testing]					
1	2.610×10^{-08}	3.400×10^{-09}	6.21×10^{-09}	2.36×10^{-08}	1.49×10^{-06}	1×10^{-09}	220	01
2	3.430×10^{-09}	3.836×10^{-09}	4.13×10^{-09}	2.69×10^{-09}	7.27×10^{-06}	1×10^{-10}	144	01
3	1.490×10^{-09}	1.570×10^{-09}	3.99×10^{-09}	9.10×10^{-10}	1.66×10^{-06}	1×10^{-10}	109	01

Table 2. Designed procedure for the FKBC model.

Data availability

All data generated or analyzed during this study are included in this article.

Received: 1 August 2023; Accepted: 14 December 2023

Published online: 20 December 2023

References

1. Arpino, G. *et al.* Gene expression profiling in breast cancer: A clinical perspective. *Breast* **22**(2), 109–120 (2013).
2. Goss, P. E. *et al.* Male breast carcinoma: A review of 229 patients who presented to the Princess Margaret Hospital during 40 years: 1955–1996. *Cancer Interdiscipl. Int. J. Am. Cancer Soc.* **85**(3), 629–639 (1999).
3. Giordano, S. H. *et al.* Breast carcinoma in men: A population-based study. *Cancer Interdiscipl. Int. J. Am. Cancer Soc.* **101**(1), 51–57 (2004).
4. Ahamedin Jemal, D. A. *et al.* Cancer statistics. 2004. *CA Cancer J. Clin.* **54**(1), 8–29 (2004).
5. Czene, K. *et al.* How to treat male breast cancer. *Breast (Edinburgh, Scotland)* **16**, S147–54 (2007).
6. Anderson, W. F. *et al.* Is male breast cancer similar or different than female breast cancer?. *Breast Cancer Res. Treat.* **83**, 77–86 (2004).
7. Miao, H. *et al.* Incidence and outcome of male breast cancer: an international population-based study. *J. Clin. Oncol.* **29**(33), 4381–4386 (2011).
8. Couch, F. J. *et al.* Inherited mutations in 17 breast cancer susceptibility genes among a large triple-negative breast cancer cohort unselected for family history of breast cancer. *J. Clin. Oncol.* **33**(4), 304 (2015).
9. McCulloch, M. *et al.* Diagnostic accuracy of canine scent detection in early-and late-stage lung and breast cancers. *Integr. Cancer Ther.* **5**(1), 30–39 (2006).
10. Fan, X. *et al.* Penetrance of breast cancer susceptibility genes from the eMERGE III network. *JNCI Cancer Spectrum* **5**(4), pkab044 (2021).
11. Mufudza, C., Walter, S. & Edward, T. C. Assessing the effects of estrogen on the dynamics of breast cancer. *Computat. Math. Methods Med.* **2012**, 1–14. <https://doi.org/10.1155/2012/473572> (2012).
12. Bray, F. *et al.* Global cancer statistics 2018: GLOBOCAN estimates of incidence and mortality worldwide for 36 cancers in 185 countries. *CA Cancer J. Clin.* **68**(6), 394–424 (2018).
13. Arshad, S. *et al.* In-silico analyses of nonsynonymous variants in the BRCA1 gene. *Biochem. Genet.* **59**(6), 1506–1526 (2021).
14. Børresen-Dale, A.-L. Genetic profiling of breast cancer: From molecular portraits to clinical utility. *Int. J. Biol. Markers* **18**(1), 54–56 (2003).
15. Cheang, M. C. U., van de Rijn, M. & Nielsen, T. O. Gene expression profiling of breast cancer. *Annu. Rev. Pathol. Mech. Dis.* **3**, 67–97 (2008).
16. Abernathy, K. *et al.* Global dynamics of a breast cancer competition model. *Differ. Equat. Dyn. Syst.* **28**, 791–805 (2020).
17. Enderling, H. *et al.* A mathematical model of breast cancer development, local treatment and recurrence. *J. Theor. Biol.* **246**(2), 245–259 (2007).
18. Solis-Pérez, J. E., Gómez-Aguilar, J. F. & Atangana, A. A fractional mathematical model of breast cancer competition model. *Chaos Solitons Fractals* **127**, 38–54 (2019).
19. Ganji, R. M. *et al.* A mathematical model and numerical solution for brain tumor derived using fractional operator. *Results Phys.* **28**, 104671 (2021).
20. Sánchez, Y. G., Zulqurnain, S. & Guirao, J. L. G. Design of a nonlinear SITR fractal model based on the dynamics of a novel coronavirus (COVID-19). *Fractals* **28**(08), 2040026 (2020).
21. Sabir, Z. *et al.* Design of a novel second-order prediction differential model solved by using adams and explicit Runge-Kutta numerical methods. *Math. Problems Eng.* **2020**, 1–7 (2020).
22. Hart, R. T., Davy, D. T. & Heiple, K. G. Mathematical modeling and numerical solutions for functionally dependent bone remodeling. *Calcified Tissue Int.* **36**, S104–S109 (1984).
23. Fogelson, A. L. A mathematical model and numerical method for studying platelet adhesion and aggregation during blood clotting. *J. Computat. Phys.* **56**(1), 111–134 (1984).
24. Sana, S. S. A structural mathematical model on two echelon supply chain system. *Ann. Oper. Res.* **315**(2), 1997–2025 (2022).
25. Oshinubi, K. *et al.* Approach to COVID-19 time series data using deep learning and spectral analysis methods. *Aims Bioeng.* **9**(1), 1–21 (2022).
26. Botmart, T. *et al.* A hybrid swarming computing approach to solve the biological nonlinear Leptospirosis system. *Biomed. Signal Process. Control* **77**, 103789 (2022).
27. Sanchez, Y.G., et al. Solving a class of biological HIV infection model of latently infected cells using heuristic approach. *Discrete Contin. Dyn. Syst. S* **14** (2018).
28. Saeed, T. *et al.* A computational approach to solve the nonlinear biological prey–predator system. *Fractals* **30**(10), 2240267 (2022).
29. Sabir, Z. *et al.* Dynamics of multi-point singular fifth-order Lane-Emden system with neuro-evolution heuristics. *Evol. Syst.* <https://doi.org/10.1007/s12530-021-09413-1> (2022).
30. Umar, M. *et al.* Heuristic computing with sequential quadratic programming for solving a nonlinear hepatitis B virus model. *Math. Comput. Simul.* **212**, 234–248 (2023).
31. Watcharaporn, C. *et al.* Artificial intelligent investigations for the dynamics of the bone transformation mathematical model. *Inform. Med. Unlock.* **34**, 101105 (2022).
32. Thongchai, B. *et al.* Stochastic investigations for the fractional vector-host diseased based saturated function of treatment model. *Comput. Mater. Continua* **75**(1), 559–573 (2023).
33. Sabir, Z. *et al.* A novel radial basis procedure for the SIRC epidemic delay differential model. *Int. J. Comput. Math.* **100**(10), 2014–2025 (2023).

34. Sabir, Z. *et al.* A swarming neural network computing approach to solve the Zika virus model. *Eng. Appl. Artif. Intell.* **126**, 106924 (2023).
35. AbuAli, N., Khan, M. B. & Sabir, Z. A computational stochastic procedure for solving the epidemic breathing transmission system. *Sci. Rep.* **13**(1), 16220 (2023).
36. Sabir, Z. Neuron analysis through the swarming procedures for the singular two-point boundary value problems arising in the theory of thermal explosion. *Eur. Phys. J. Plus* **137**(5), 638 (2022).
37. Sabir, Z., Said, S. B. & Al-Mdallal, Q. Hybridization of the swarming and interior point algorithms to solve the Rabinovich-Fabrikant system. *Sci. Rep.* **13**(1), 10932 (2023).
38. Sabir, Z. & Said, S. B. A fractional order nonlinear model of the love story of Layla and Majnun. *Sci. Rep.* **13**(1), 5402 (2023).
39. Sabir, Z. Stochastic numerical investigations for nonlinear three-species food chain system. *Int. J. Biomath.* **15**(04), 2250005 (2022).
40. Yang, X.-J., Ragulskis, M. & Tana, T. A new general fractional-order derivative with Rabotnov fractional-exponential kernel. *Therm. Sci.* **23**(6B), 3711–3718 (2019).
41. Kamal, S. *et al.* Semi-analytical study of Pine Wilt Disease model with convex rate under Caputo–Febrizio fractional order derivative. *Chaos Solitons Fractals* **135**, 109754 (2020).
42. Owolabi, K. M. & Hammouch, Z. Spatiotemporal patterns in the Belousov-Zhabotinskii reaction systems with Atangana-Baleanu fractional order derivative. *Phys. A Stat. Mech. Appl.* **523**, 1072–1090 (2019).
43. Yongsheng, H. *et al.* Application of fractional-order derivative in the quantitative estimation of soil organic matter content through visible and near-infrared spectroscopy. *Geoderma* **337**, 758–769 (2019).
44. Ghanbari, B. & Djilali, S. Mathematical and numerical analysis of a three-species predator-prey model with herd behavior and time fractional-order derivative. *Math. Methods Appl. Sci.* **43**(4), 1736–1752 (2020).
45. El Hayek, P., Boueri, M., Nasr, L., Aoun, C., Sayad, E. and Jallad, K., (2023). Cholera Infection Risks and Cholera Vaccine Safety in Pregnancy. *Infectious Diseases in Obstetrics and Gynecology*, 2023.
46. Issa, J. S. A nonlinear absorber for the reflection of travelling waves in bars. *Nonlinear Dyn.* **108**(4), 3279–3295 (2022).
47. Tian, M., El Khoury, R. & Alshater, M. M. The nonlinear and negative tail dependence and risk spillovers between foreign exchange and stock markets in emerging economies. *J. Int. Financial Mark. Inst. Money* **82**, 101712 (2023).
48. Kassis, M.T., Tannir, D., Toukhtarian, R. and Khazaka, R., (2019), October. Moments-based sensitivity analysis of x-parameters with respect to linear and nonlinear circuit components. In 2019 IEEE 28th Conference on Electrical Performance of Electronic Packaging and Systems (EPEPS) (pp. 1–3). IEEE.
49. Abi Younes, G. & El Khatib, N. Mathematical modeling of atherosclerosis: Atheroprotective role of HDL. *J. Theor. Biol.* **529**, 110855 (2021).
50. Habre, S. S. Qualitative aspects of differential equations in an inquiry-oriented course. *Int. J. Math. Educ. Sci. Technol.* **54**(3), 351–364 (2023).
51. Abi Younes, G. & El Khatib, N. Mathematical modeling of inflammatory processes of atherosclerosis. *Math. Model. Nat. Phenomena* **17**, 5 (2022).
52. Touma, R. & Saleh, M. A. Well-balanced central schemes for pollutants transport in shallow water equations. *Math. Comput. Simul.* **190**, 1275–1293 (2021).
53. Younes, Y., Hallit, S. & Obeid, S. Premenstrual dysphoric disorder and childhood maltreatment, adulthood stressful life events and depression among Lebanese university students: A structural equation modeling approach. *BMC Psychiatry* **21**(1), 1–10 (2021).
54. Habre, S. Inquiry-oriented differential equations: A guided journey of learning. *Teach. Math. Appl. Int. J. IMA* **39**(3), 201–212 (2020).
55. Ghanem, C. A. *et al.* Gay community integration as both a source of risk and resilience for HIV prevention in Beirut. *Int. J. Behav. Med.* **27**, 160–169 (2020).
56. Kmeid, J. *et al.* Active Mycobacterium tuberculosis infection at a comprehensive cancer center, 2006–2014. *BMC Infect. Dis.* **19**, 1–8 (2019).
57. Mahdi, A. *et al.* Severe acute respiratory syndrome coronavirus 2 antibody seroprevalence in Lebanon: A population-based cross-sectional study. *IJID Reg.* **2**, 184–190 (2022).
58. Nasrallah, S. *et al.* Pharmacological treatment in pregnant women with moderate symptoms of coronavirus disease 2019 (COVID-19) pneumonia. *J. Matern.-Fetal Neonatal Med.* **35**(25), 5970–5977 (2022).
59. Chirinos, J. A. *et al.* A randomized clinical trial of lipid metabolism modulation with fenofibrate for acute coronavirus disease 2019. *Nat. Metabol.* **4**(12), 1847–1857 (2022).
60. Obeid, S., Sacre, H., Hallit, S. & Salameh, P. School bullying—The silent epidemic: A cross-sectional study of factors associated with peer victimization among lebanese adolescents. *J. Interpers. Violence* **37**(1–2), NP1147–NP1169 (2022).
61. Al-Abbas, M. *et al.* Toward an improvement of engineering teaming skills through an in-house professionalism course. *IEEE Trans. Educ.* **63**(4), 273–282 (2020).
62. Alam, M. M. *et al.* Comparative dynamics of mixed convection heat transfer under thermal radiation effect with porous medium flow over dual stretched surface. *Sci. Rep.* **13**(1), 12827 (2023).

Acknowledgment

The authors are thankful to the Deanship of Scientific Research, King Khalid University, Abha, Saudi Arabia, for financially supporting this work through the General Research Project under Grant No: RGP.1/435/44.

Author contributions

M.A. devised the project, the main conceptual ideas and proof outline. Z.H and Q.H. worked out almost all of the technical details and performed the numerical calculations for the suggested experiment. Z.S. and B.K.S. worked out the bound for quantum mechanics, with help from M.M.A. and Z.S. verified the numerical results by an independent implementation. M.A., Q.H. and Z.S. proposed the model experiment in discussions with all authors and Z.H. and Z.S. wrote the manuscript. Additionally, M.A., Q.H., Z.S. and Z.H. validated the numerical results and revised the manuscript.

Competing interests

The authors declare no competing interests.

Additional information

Correspondence and requests for materials should be addressed to Z.H. or M.A.

Reprints and permissions information is available at www.nature.com/reprints.

Publisher's note Springer Nature remains neutral with regard to jurisdictional claims in published maps and institutional affiliations.



Open Access This article is licensed under a Creative Commons Attribution 4.0 International License, which permits use, sharing, adaptation, distribution and reproduction in any medium or format, as long as you give appropriate credit to the original author(s) and the source, provide a link to the Creative Commons licence, and indicate if changes were made. The images or other third party material in this article are included in the article's Creative Commons licence, unless indicated otherwise in a credit line to the material. If material is not included in the article's Creative Commons licence and your intended use is not permitted by statutory regulation or exceeds the permitted use, you will need to obtain permission directly from the copyright holder. To view a copy of this licence, visit <http://creativecommons.org/licenses/by/4.0/>.

© The Author(s) 2023